Optics Communications 476 (2020) 126329

Contents lists available at ScienceDirect

Optics Communications

journal homepage: www.elsevier.com/locate/optcom

All-fiberized, mode-locked laser at 1.95 μm using copper chalcogenide Cu_2Te-based evanescent field interaction

H. Ahmad [a,b,*], S.N. Aidit [a], N. Yusoff [a], N.N. Ismail [a], M.F. Ismail [a], A.K. Zamzuri [c], K. Thambiratnam [a]

[a] Photonics Research Centre, University of Malaya, 50603 Kuala Lumpur, Malaysia
[b] Physics Dept., Faculty of Science, University of Malaya, 50603 Kuala Lumpur, Malaysia
[c] Department of Physics, Kulliyyah of Science, International Islamic University Malaysia, 25200 Kuantan, Pahang, Malaysia

ARTICLE INFO

Keywords:
Copper chalcogenide
Saturable absorber
Mode-locked
Thulium
Fiber laser

ABSTRACT

For the first time, a copper telluride (Cu_2Te) based saturable absorber (SA) was demonstrated for mode-locking in a thulium-doped fiber laser. Layers of Cu_2Te were deposited onto a side polished fiber (SPF) using the optical deposition technique, forming an all-fiber SA device. The nonlinear optical properties of the SA device were investigated based on the balanced twin-detector measurement scheme. The Cu_2Te-deposited SPF SA was capable of generating stable soliton mode-locked pulses with a pulse duration of 1.58 ps at a center wavelength of 1951 nm with a signal to noise ratio (SNR) of more than 60 dB, as well as a peak power of 250 mW and a pulse energy of 0.39 nJ.

1. Introduction

Soliton lasers operating at the 2 μm region are promising light sources and have received wide research interest due to their versatile applications in long-range light detection and ranging (LIDAR), laser surgery, material processing and laser spectroscopy [1–4]. Mode-locked fiber lasers are simple and exhibit significant reliability and environmental stability as compared to free-space optics-based lasers. Optical fiber-based 2 μm lasers use thulium (Tm) [5], holmium (Ho) [6] or Tm–Ho co-doped fibers [7] as the primary gain medium. Various active/passive schemes have been employed in fiber lasers to generate mode-locked pulses in the picoseconds and femtosecond range [8]. In contrast to active scheme which requires external and complicated device [9–11], passive scheme offers advantages of a compact, flexible and cost-effective mode-locked system through the use of nonlinear optical element, called a saturable absorber (SA).

Two-dimensional (2D) materials such as graphene [12–15], black phosphorus (BP) [16–18] and topological insulators (TIs) [19–21] have been widely employed as SAs for demonstrating passively mode-locked fiber laser owing to their high optical nonlinearity property, broadband saturable absorption and ultrafast carrier dynamics. Nevertheless, the aforementioned materials have some drawbacks. For example, graphene possesses weak light–matter interaction due to its low modulation depth (typically ~1.2% per layer [22]), whereas BP can be easily oxidized when exposed to a humid environment [23]. Therefore, the exploration of new SAs has always attracted a lot of attention. Recently, transition metal dichalcogenides (TMDs), including MoS_2, WS_2, $MoSe_2$ WSe_2 and ReS_2 [24–29] have been widely employed as SAs due to their advantages of wide absorption range and its exotic optical and electrical properties which are different from their bulk counterpart. More recently, binary chalcogenide semiconductors which arises as a result of quantum confinement effect have received substantial attention due to their size-dependent optical and physical properties. Copper chalcogenides have been widely used as solar cells, optical recording materials and optical filters. This group of materials possesses an interesting localized surface plasmon resonance (LSPR) effect in the near infrared (NIR), which is very useful for surface-enhanced Raman scattering (SERS) and photoacoustic imaging applications [30]. Of these copper chalcogenides, copper telluride (Cu_xTe) in particular is attractive for a wide range of applications owing to its direct bandgap ranging from 1.1 eV to 1.5 eV [29] as well as large thermoelectric power. Cu_xTe has a wide range of compositions with each composition having a different crystal structure, depending on the value of x ($1 < x < 2$). For instance, the Cu_2Te has an optical band gap of 1.1 eV [31]. The SA device based on the evanescent wave interaction has drawn extensive attention in demonstrating mode-locked fiber laser due to its robustness, large nonlinear interaction length, high degree of compatibility to the SMF and low optically induced thermal damage [32]. Various 2D materials have been utilized to enable mode-locking operation through the nonlinear interaction with evanescent field [25,33–39]. However, the saturable absorption properties of copper chalcogenides have been

* Corresponding author at: Photonics Research Centre, University of Malaya, 50603 Kuala Lumpur, Malaysia.
E-mail address: harith@um.edu.my (H. Ahmad).

https://doi.org/10.1016/j.optcom.2020.126329
Received 5 June 2020; Received in revised form 21 July 2020; Accepted 25 July 2020
Available online 28 July 2020
0030-4018/© 2020 Elsevier B.V. All rights reserved.

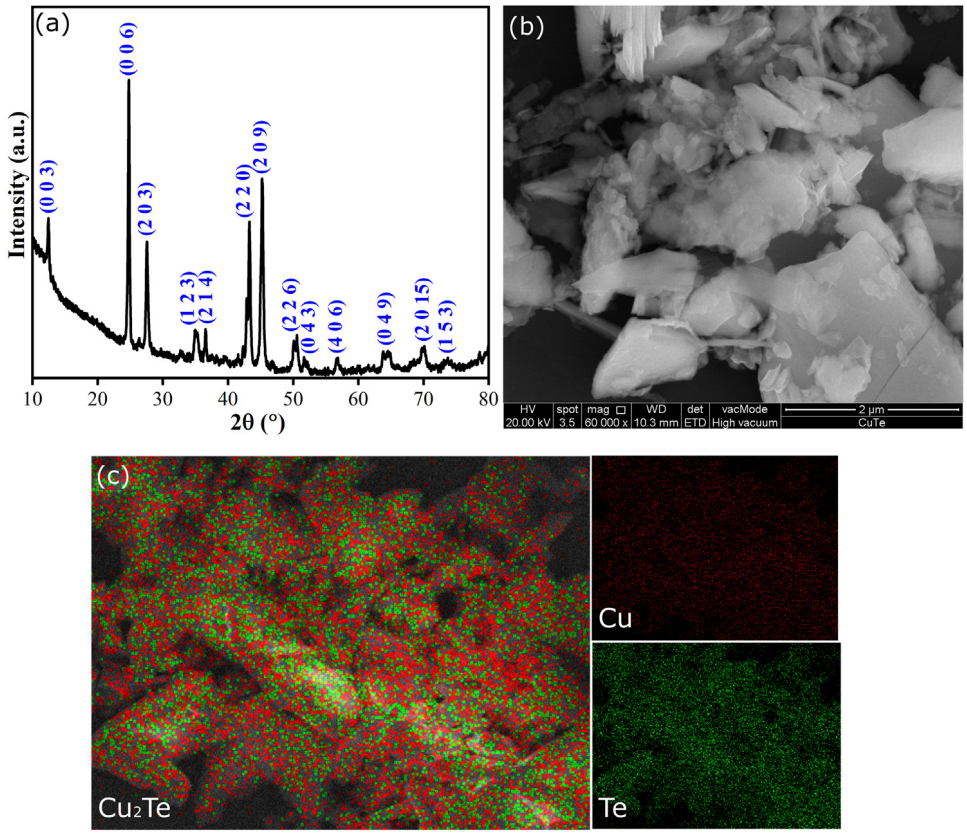

Fig. 1. Characterization of Cu_2Te (a) XRD spectrum; (b) FESEM image; and (c) selected area EDX elemental mapping.

investigated. Thus, in this work, a Cu_2Te-based evanescent field interaction is demonstrated to produce mode-locked pulses. The Cu_2Te is synthesized using simple solution method and deposited on the side polished fiber (SPF) using optical deposition method. By utilizing the Cu_2Te-deposited SPF, stable picoseconds soliton pulses are delivered from the Tm-doped fiber laser (TDFL) with >60 dB of signal-to-noise ratio (SNR). At maximum pump power of 462 mW, the laser average output power is 3.2 mW, with a corresponding pulse energy and peak power of about 0.39 nJ and 250 W. This is the first time, to the best of the author's knowledge, of the use of a Cu_2Te on a SPF as an SA. This work proposed a practical photonic device which may find wide applications in ultrafast photonics.

2. Cu_2Te-deposited side polished fiber fabrication and characterization

A Cu_2Te powder was purchased from 2D Semiconductors, while polyvinyl alcohol (PVA, M_W ~31,000) was bought from Sigma Aldrich. All chemicals are used as received without further purification. The Cu_2Te was synthesized using a simple solution method. Initially, 100 mg of Cu_2Te powder was dispersed in 10 ml of deionized (DI) water. The dispersion was sonicated in a bath sonicator for 10 h at room temperature to form a homogeneous solution. In order to remove large agglomerations, the Cu_2Te dispersion was then centrifuged at 4000 rpm for 10 min and the supernatant was collected.

The X-ray diffraction (XRD) investigation was carried out using a Malvern Panalytical Empyrean, recorded in the range of $2\theta = 5 - 70°$. The XRD pattern obtained from the Cu_2Te powder is depicted in Fig. 1(a). A few sharp peaks can be observed in the XRD spectrum of Cu_2Te located at 2θ of 12.45, 24.80, 27.55, 43.48, and 45.23° which corresponds to the (0 0 3), (0 0 6), (2 0 3), (2 2 0), and (2 0 9) planes that matched with the standard diffraction pattern of hexagonal Cu_2Te (JCPDS 96-901-1862). The existence of the sharp peaks and the absence of impurity peaks indicate the high crystallinity and purity of Cu_2Te. The surface morphology and the energy dispersive X-ray (EDX) elemental mapping analysis of Cu_2Te were investigated using a JEOL JSM 7600F field emission scanning electron microscope (FESEM) together with an EDX. It is evident from the FESEM image presented in Fig. 1(b) that the Cu_2Te is composed of few flake-like sheets that overlap with one another and the flakes size is mainly ~1 µm. The EDX elemental mapping images of individual copper (Cu) and tellurium (Te) as well as the overlay image of these two elements are illustrated in Fig. 1(c). It is noteworthy that the Cu_2Te consists of Cu and Te elements, hence further confirming the formation of Cu_2Te.

After the successful exfoliation of the Cu_2Te powder, the Cu_2Te-deposited SPF was fabricated and its saturable absorption properties was investigated. The Cu_2Te sheets were transferred onto the polished region of the commercial SPF (Phoenix Photonics) using the optical deposition method. The polished region area had a dimension of 17 mm in length and width of about 125 µm (the diameter of the cladding). This area is about 2 µm above the core-cladding interface. Slow evaporation at ambient temperature resulted in the Cu_2Te-deposited SPF, as shown in Fig. 2(a). The saturable absorption of the device was realized through the nonlinear interaction of the Cu_2Te sheets with the evanescence field of light in the SPF. The existence of the evanescent field in the SPF can be observed by injecting the visible light, as shown in the inset of Fig. 2(b). The nonlinear saturable absorption of the Cu_2Te-deposited SPF was investigated based on a balanced twin-detector measurement method. The measurement was carried out using a commercial ELMO femtosecond laser (central wavelength: 1560 nm, repetition rate: 100 MHz, pulse duration: ~150 fs). The intensity dependent absorption is fitted by $\alpha(I) = \left[\frac{\Delta\alpha}{1+\left(\frac{I}{I_{sat}}\right)}\right] + \alpha_{ns}$, where $\Delta\alpha$, I_{sat} and α_{ns} represent modulation depth, saturation intensity and non-saturable loss, respectively. The modulation depth of the SA was measured to be 25%, whereas the

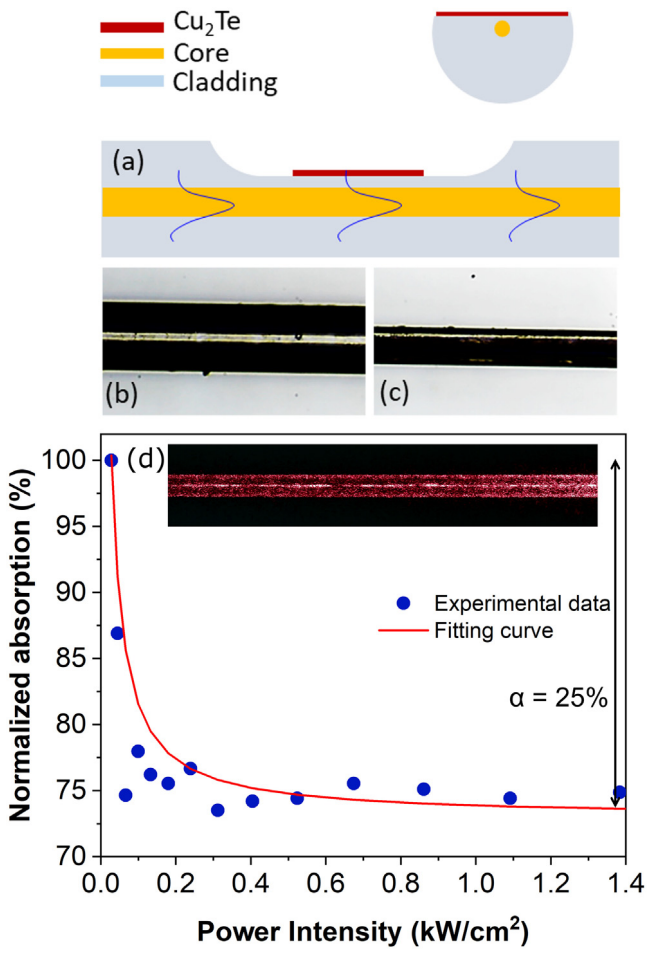

Fig. 2. (a) Illustration of the Cu_2Te-deposited SPF; (b) photomicrograph of SPF before and (c) after polished; and (d) nonlinear absorption curve. Inset shows the evanescent field from SPF after injecting with red light source. . (For interpretation of the references to color in this figure legend, the reader is referred to the web version of this article.)

saturation intensity is 0.08 kW/cm^2 which corresponded to the peak power of 0.025 mW and silica fiber cross-sectional area of 3.24×10^{-7} cm^2.

3. Experimental setup

A ring TDFL cavity was constructed to generate mode-locked pulses in 2.0 μm region as shown in Fig. 3. In order to achieve this, the Cu_2Te-deposited SPF was incorporated in the TDFL cavity. The thulium-doped fiber amplifier consists of a piece of 4 m TmDF200 thulium-doped fiber (TDF) with a group velocity dispersion (GVD) parameter of −21.9 ps^2/km at 1940 nm and peak absorption of 20 dB/m at 1550 nm. The TDF was dual-pumped by 1550 nm laser diodes (LDs) through the 1550 nm ports of two 1550/2000 wavelength division multiplexers (WDMs). In addition to the fiber amplifier, the cavity consists of an isolator (ISO) to force unidirectional operation of the ring cavity, polarization controller (PC) to adjust the polarization state of the circulating light. A 90:10 fiber-pigtailed optical coupler (OC) was added to the cavity for temporal and optical analysis. All of the fibers in the cavity, with the exception of the TDF, constitute of single mode fibers (SMF-28s) with a GVD of −71.4 ps^2/km at 1940 nm. The total cavity length was 25.5 m and net cavity dispersion is estimated as −1.62 ps^2 (anomalous dispersion). The performance of the laser was examined using an Yokogawa AQ6375 optical spectrum analyser

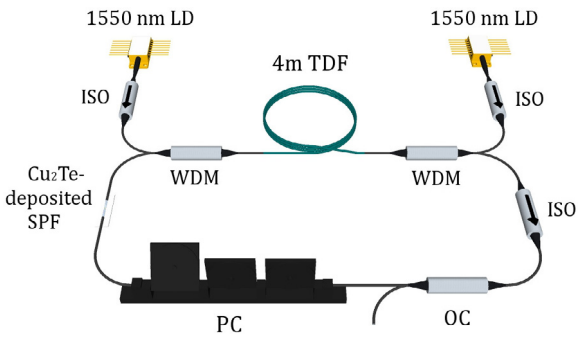

Fig. 3. Experimental setup of the passively mode-locked TDFL.

(OSA), a 5 GSa/s Rohde & Schwarz RTM3002 oscilloscope (OSC) and a 7.8 GHz Anritsu MS2683A radio frequency spectrum analyser (RFSA) coupled with a 10 GHz photodetector and an optical autocorrelator (APE PulseCheck).

4. Results and discussion

By carefully adjusting the PC in the laser cavity, stable mode-locked pulse train was observed at threshold pump power of 87 mW. The pulse train as shown in Fig. 4(a) was observed at pulse repetition frequency of 8.1 MHz, which corresponds well to the cavity round trip time of 124 ns. This verifies the fundamental operation of the mode-locked laser. Fig. 4(b) shows the enlarged optical spectrum of the generated pulses, centered at 1951 nm with a full-width half maximum (FWHM) of 2.6 nm. As seen from the inset of Fig. 4(b), Kelly sidebands were observed which are characteristic of an all-anomalous dispersion or solitonic mode-locked laser. The autocorrelation trace as shown in Fig. 4(c) is well-fitted with a Sech^2 profile, showing a deconvolved pulse duration of 1.58 ps.

The time-bandwidth product is 0.323, which is just slightly higher than the theoretical limit of 0.315, indicating that the laser cavity has a low chirp. Fig. 4(d) depicts the radio frequency spectrum measured around fundamental frequency with a resolution bandwidth (RBW) of 300 Hz. A sharp and clean peak is observed at 8.1 MHz with SNR of >60 dB, demonstrating good mode-locking operation. RF spectrum, on a wider range span of 1 GHz as shown in the inset is observed free from spectral modulation, indicating no Q-switching mode-locking. Fig. 5 shows the average output power as a function of pump power. At the maximum pump power of 462 mW, the laser average output power was measured around 3.2 mW, with a peak power of 250 W and a pulse energy of 0.39 nJ. The pulse energy as measured in this work is high with no pulse splitting observed. This could be explained using the soliton area theorem [40], where mode-locked fiber lasers operating at 2 μm can typically support high energy soliton pulse due to the low nonlinearity and large dispersion of silica fiber. Besides, the use of evanescent-wave-type SA such as SPF can also be important factor to enhance the soliton pulse energy [12,41,42]. A slope efficiency of 0.8% was obtained from this laser. The low power efficiency could arise from the high non-saturable loss of the Cu_2Te-deposited SPF, possibly due to the large polishing depth and roughness of the polished surface which would result in severe scattering losses. On top of this, there are also losses from the components used in the cavity, which will also reduce the efficiency of the laser.

The long-term stability of the mode-locking operation was further evaluated by observing the output spectrum for 4 h. The output spectrum was recorded every 30 mins over a period of 4 h under fixed experimental condition such as pump power of 192 mW, as shown in Fig. 6(a). Neither the center wavelength drifted nor a new wavelength component was generated during the measurement period. Moreover, no significant degradation of the optical spectra is observed,

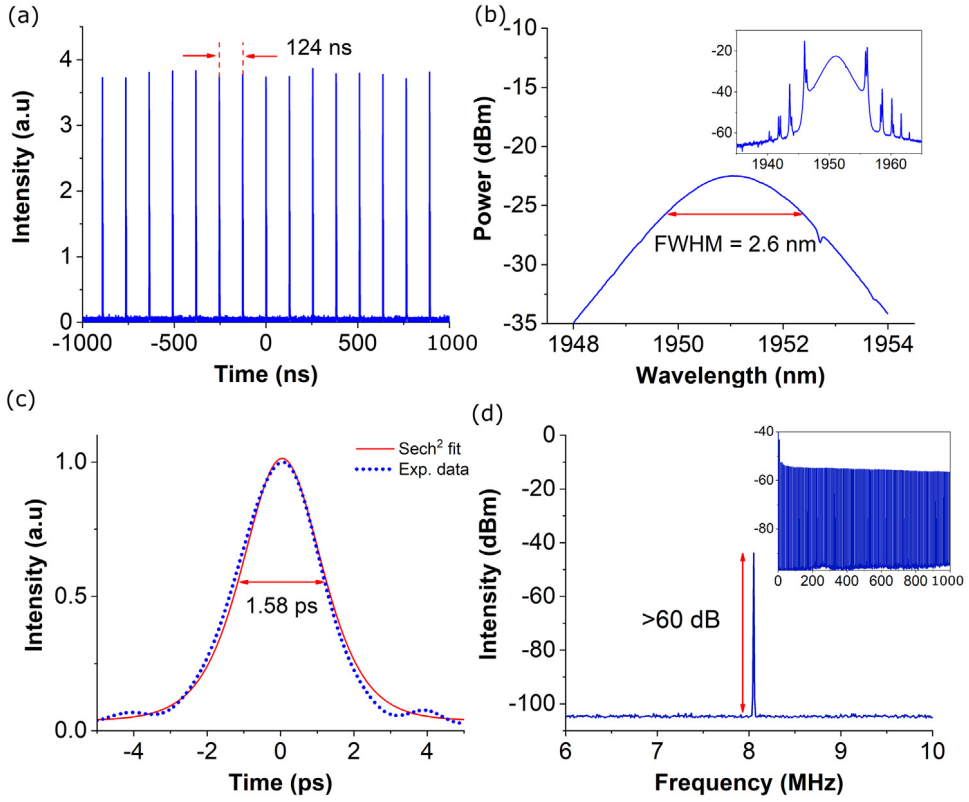

Fig. 4. (a) Mode-locked pulse train; (b) enlarged optical spectrum with FWHM of 2.6 nm. Inset shows full soliton spectrum; (c) autocorrelation trace with a Sech^2 fit; and (d) radio frequency spectrum, on a 10 MHz range span with a 300 Hz RBW measured around fundamental frequency of 8.1 MHz. Inset shows spectrum on wider span range of 1 GHz.

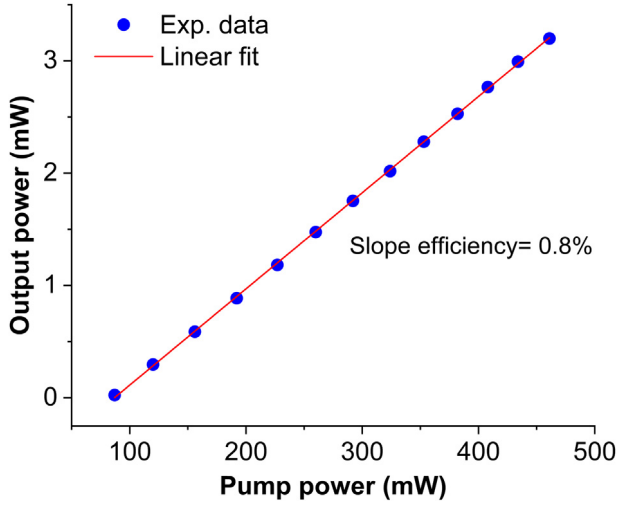

Fig. 5. Average output power against pump power.

as shown in Fig. 6(b). This verifies that the mode-locking operation possesses excellent repeatability and long-term stability. In order to ensure the mode-locking operation in the TDFL was induced by the Cu_2Te-deposited SPF, a polarization dependent loss (PDL) measurement was performed. The PDL of the SA device was measured around 0.2 dB, which was low enough to exclude nonlinear polarization rotation (NPR) effect [43]. This was further confirmed by removing the SA and placing an SPF with no material coating. In this case no mode-locking was observed. The generation of stable soliton pulses using Cu_2Te-deposited SPF in 2 μm region has clearly indicated the performance of the copper chalcogenide as an effective SA.

5. Conclusions

A passively mode-locked TDFL based on copper chalcogenide was demonstrated for the first time. The mode-locked pulses were obtained based on the evanescent field interaction, where the Cu_2Te was deposited onto a SPF. The pulsed laser had a repetition rate of 8.1 MHz and a pulse width of 1.58 ps, as well as a pulse energy of 0.39 nJ and a peak power of 250 W. The RF spectrum of the laser indicated good stability with an SNR of more than 60 dB. The laser was also stable when tested for a long-term stability, showing no sign of instability for a period of 4 h. The mode-locked TDFL operating in the 2 μm wavelength region would have useful applications in the medical field and as sensors.

Declaration of competing interest

The authors declare that they have no known competing financial interests or personal relationships that could have appeared to influence the work reported in this paper.

Acknowledgments

This work was supported by the Ministry of Higher Education, Malaysia [Grant Number HiCoE Phase II Funding] and the University of Malaya [Grant Number RU 011 – 2019 and RK021 – 2019].

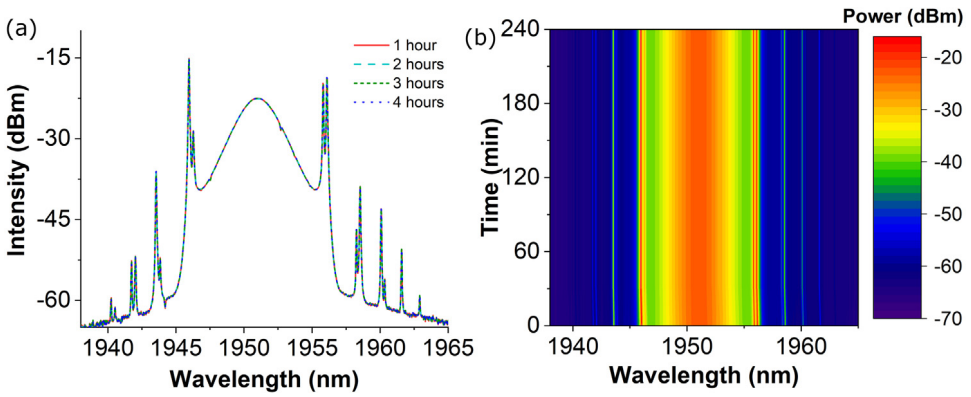

Fig. 6. (a) Spectra acquired after 1-h (red line), 2 h (cyan dash line), 3 h (green short dash line) and 4 h (blue dot line); and (b) 3D spectrum of mode-locking operation over 240 min. (For interpretation of the references to color in this figure legend, the reader is referred to the web version of this article.)

References

[1] C.W. Rudy, M.J.F. Digonnet, R.L. Byer, Advances in 2-μm Tm-doped mode-locked fiber lasers, Opt. Fiber Technol. 20 (2014) 642–649.

[2] W. Zeller, L. Naehle, P. Fuchs, F. Gerschuetz, L. Hildebrandt, J. Koeth, DFB lasers between 760 nm and 16 μm for sensing applications, Sensors 10 (2010) 2492–2510.

[3] N.M. Fried, K.E. Murray, High-power thulium fiber laser ablation of urinary tissues at 1.94 μm, J. Endourol. 19 (2005) 25–31.

[4] I. Mingareev, F. Weirauch, A. Olowinsky, L. Shah, P. Kadwani, M. Richardson, Welding of polymers using a 2 μm thulium fiber laser, Opt. Laser Technol. 44 (2012) 2095–2099.

[5] Z. Li, A.M. Heidt, J.M.O. Daniel, Y. Jung, S.U. Alam, D.J. Richardson, Thulium-doped fiber amplifier for optical communications at 2 μm, Opt. Express 21 (2013) 9289–9297.

[6] S.O. Antipov, A.S. Kurkov, A holmium-doped fiber amplifier at 2.1 μm, Laser Phys. Lett. 10 (2013) 125106.

[7] J. Lee, J.H. Lee, Femtosecond Tm–Ho co-doped fiber laser using a bulk-structured Bi2Se3 topological insulator, Chin. Phys. B 27 (2018) 94219.

[8] S.W. Harun, R. Akbari, H. Arof, H. Ahmad, Mode-locked bismuth-based erbium-doped fiber laser with stable and clean femtosecond pulses output, Laser Phys. Lett. 8 (2011) 449.

[9] J. Kim, J. Koo, J.H. Lee, All-fiber acousto-optic modulator based on a cladding-etched optical fiber for active mode-locking, Photonics Res. 5 (2017) 391–395.

[10] M. Bello-Jiménez, E. Hernández-Escobar, A. Camarillo-Avilés, O. Pottiez, A. Díez, M.V. Andrés, Actively mode-locked all-fiber laser by 5 MHz transmittance modulation of an acousto-optic tunable bandpass filter, Laser Phys. Lett. 15 (2018) 85113.

[11] J. Kim, J. Koo, J.H. Lee, An actively mode-locked, all fiber laser using an acousto-optic modulator based on cladding-etched optical fiber, in: Adv. Solid State Lasers, Optical Society of America, 2017, pp. JM5A–23.

[12] M. Zhang, E.J.R. Kelleher, F. Torrisi, Z. Sun, T. Hasan, D. Popa, F. Wang, A.C. Ferrari, S.V. Popov, J.R. Taylor, Tm-doped fiber laser mode-locked by graphene-polymer composite, Opt. Express 20 (2012) 25077–25084.

[13] H. Zhang, D.Y. Tang, L.M. Zhao, Q.L. Bao, K.P. Loh, B. Lin, S.C. Tjin, Compact graphene mode-locked wavelength-tunable erbium-doped fiber lasers: from all anomalous dispersion to all normal dispersion, Laser Phys. Lett. 7 (2010) 591.

[14] Z. Sun, T. Hasan, F. Torrisi, D. Popa, G. Privitera, F. Wang, F. Bonaccorso, D.M. Basko, A.C. Ferrari, Graphene mode-locked ultrafast laser, ACS Nano. 4 (2010) 803–810.

[15] D. Popa, Z. Sun, F. Torrisi, T. Hasan, F. Wang, A.C. Ferrari, Sub 200 fs pulse generation from a graphene mode-locked fiber laser, Appl. Phys. Lett. 97 (2010) 203106.

[16] J. Li, H. Luo, B. Zhai, R. Lu, Z. Guo, H. Zhang, Y. Liu, Black phosphorus: a two-dimension saturable absorption material for mid-infrared Q-switched and mode-locked fiber lasers, Sci. Rep. 6 (2016) 30361.

[17] J. Sotor, G. Sobon, M. Kowalczyk, W. Macherzynski, P. Paletko, K.M. Abramski, Ultrafast thulium-doped fiber laser mode locked with black phosphorus, Opt. Lett. 40 (2015) 3885–3888.

[18] X. Jin, G. Hu, M. Zhang, Y. Hu, T. Albrow-Owen, R.C.T. Howe, T.-C. Wu, Q. Wu, Z. Zheng, T. Hasan, 102 fs pulse generation from a long-term stable, inkjet-printed black phosphorus-mode-locked fiber laser, Opt. Express 26 (2018) 12506–12513.

[19] Y.-H. Lin, S.-F. Lin, Y.-C. Chi, C.-L. Wu, C.-H. Cheng, W.-H. Tseng, J.-H. He, C.-I. Wu, C.-K. Lee, G.-R. Lin, Using n-and p-type Bi_2Te_3 topological insulator nanoparticles to enable controlled femtosecond mode-locking of fiber lasers, Acs Photonics 2 (2015) 481–490.

[20] Z.-C. Luo, M. Liu, H. Liu, X.-W. Zheng, A.-P. Luo, C.-J. Zhao, H. Zhang, S.-C. Wen, W.-C. Xu, 2 GHz passively harmonic mode-locked fiber laser by a microfiber-based topological insulator saturable absorber, Opt. Lett. 38 (2013) 5212–5215.

[21] F. Bernard, H. Zhang, S.-P. Gorza, P. Emplit, Towards mode-locked fiber laser using topological insulators, in: Nonlinear Photonics, Optical Society of America, 2012, pp. NTh1A–5.

[22] H.-H. Kuo, S.-F. Hong, Nanographene-based saturable absorbers for ultrafast fiber lasers, J. Nanomater. 2014 (2014).

[23] Y. Huang, J. Qiao, K. He, S. Bliznakov, E. Sutter, X. Chen, D. Luo, F. Meng, D. Su, J. Decker, Interaction of black phosphorus with oxygen and water, Chem. Mater. 28 (2016) 8330–8339.

[24] H. Ahmad, M. Suthaskumar, Z.C. Tiu, A. Zarei, S.W. Harun, Q-switched Erbium-doped fiber laser using $MoSe_2$ as saturable absorber, Opt. Laser Technol. 79 (2016) 20–23.

[25] J. Du, Q. Wang, G. Jiang, C. Xu, C. Zhao, Y. Xiang, Y. Chen, S. Wen, H. Zhang, Ytterbium-doped fiber laser passively mode locked by few-layer Molybdenum Disulfide (MoS_2) saturable absorber functioned with evanescent field interaction, Sci. Rep. 4 (2014) 6346.

[26] H. Ahmad, N.E. Ruslan, M.A. Ismail, S.A. Reduan, C.S.J. Lee, S. Sathiyan, S. Sivabalan, S.W. Harun, Passively Q-switched erbium-doped fiber laser at C-band region based on WS_2 saturable absorber, Appl. Opt. 55 (2016) 1001–1005.

[27] K. Wu, X. Zhang, J. Wang, X. Li, J. Chen, WS_2 as a saturable absorber for ultrafast photonic applications of mode-locked and Q-switched lasers, Opt. Express 23 (2015) 11453–11461.

[28] B. Chen, X. Zhang, K. Wu, H. Wang, J. Wang, J. Chen, Q-switched fiber laser based on transition metal dichalcogenides MoS_2, $MoSe_2$, WS_2, and WSe_2, Opt. Express 23 (2015) 26723–26737.

[29] S. Kashida, W. Shimosaka, M. Mori, D. Yoshimura, Valence band photoemission study of the copper chalcogenide compounds, Cu_2S, Cu_2Se and Cu_2Te, J. Phys. Chem. Solids 64 (2003) 2357–2363.

[30] C. Han, Y. Bai, Q. Sun, S. Zhang, Z. Li, L. Wang, S. Dou, Ambient aqueous growth of Cu_2Te nanostructures with excellent electrocatalytic activity toward sulfide redox shuttles, Adv. Sci. 3 (2016) 1500350.

[31] S. Fonash, Solar Cell Device Physics, Elsevier, 2012.

[32] S.W. Harun, K.S. Lim, C.K. Tio, K. Dimyati, H. Ahmad, Theoretical analysis and fabrication of tapered fiber, Optik 124 (2013) 538–543.

[33] Y.-W. Song, S.-Y. Jang, W.-S. Han, M.-K. Bae, Graphene mode-lockers for fiber lasers functioned with evanescent field interaction, Appl. Phys. Lett. 96 (2010) 51122.

[34] J. Sotor, G. Sobon, K. Grodecki, K.M. Abramski, Mode-locked erbium-doped fiber laser based on evanescent field interaction with Sb_2Te_3 topological insulator, Appl. Phys. Lett. 104 (2014) 251112.

[35] Y.-W. Song, S. Yamashita, C.S. Goh, S.Y. Set, Carbon nanotube mode lockers with enhanced nonlinearity via evanescent field interaction in D-shaped fibers, Opt. Lett. 32 (2007) 148–150.

[36] M. Jung, J. Koo, P. Debnath, Y.-W. Song, J.H. Lee, A mode-locked 1.91 μm fiber laser based on interaction between graphene oxide and evanescent field, Appl. Phys. Express 5 (2012) 112702.

[37] X. Li, X. Yu, Z. Sun, Z. Yan, B. Sun, Y. Cheng, X. Yu, Y. Zhang, Q.J. Wang, High-power graphene mode-locked tm/ho co-doped fiber laser with evanescent field interaction, Sci. Rep. 5 (2015) 16624.

[38] N.H. Park, H. Jeong, S.Y. Choi, M.H. Kim, F. Rotermund, D.-I. Yeom, Monolayer graphene saturable absorbers with strongly enhanced evanescent-field interaction for ultrafast fiber laser mode-locking, Opt. Express 23 (2015) 19806–19812.

[39] M. Jung, J. Lee, J. Park, J. Koo, Y.M. Jhon, J.H. Lee, Mode-locked, 1.94-μm, all-fiberized laser using WS_2-based evanescent field interaction, Opt. Express 23 (2015) 19996–20006.

[40] L.E. Nelson, D.J. Jones, K. Tamura, H.A. Haus, E.P. Ippen, Ultrashort-pulse fiber ring lasers., Appl. Phys. B Lasers Opt. 65 (1997).
[41] H. Jeong, S.Y. Choi, M.H. Kim, F. Rotermund, Y.-H. Cha, D.-Y. Jeong, S.B. Lee, K. Lee, D.-I. Yeom, All-fiber Tm-doped soliton laser oscillator with 6 nj pulse energy based on evanescent field interaction with monoloayer graphene saturable absorber, Opt. Express 24 (2016) 14152–14158.
[42] Y.-W. Song, S. Yamashita, S. Maruyama, Single-walled carbon nanotubes for high-energy optical pulse formation, Appl. Phys. Lett. 92 (2008) 21115.
[43] J. Sotor, G. Sobon, K.M. Abramski, Sub-130 fs mode-locked Er-doped fiber laser based on topological insulator, Opt. Express 22 (2014) 13244–13249.